

Supplement of The Cryosphere, 9, 1481–1504, 2015
<http://www.the-cryosphere.net/9/1481/2015/>
doi:10.5194/tc-9-1481-2015-supplement
© Author(s) 2015. CC Attribution 3.0 License.



Supplement of

Recent changes in north-west Greenland climate documented by NEEM shallow ice core data and simulations, and implications for past-temperature reconstructions

V. Masson-Delmotte et al.

Correspondence to: V. Masson-Delmotte (valerie.masson@lsce.ipsl.fr)

The copyright of individual parts of the supplement might differ from the CC-BY 3.0 licence.

Contents:

- Supplementary tables S1-S5 describing correlation statistics between NEEM records and other records.
- Figure S1 describing the characteristics of the first principal component of Greenland accumulation records.
- Figure S2 showing the response of NEEM records to volcanic eruptions.

***Table S1.** Correlation statistics between NEEM annual $\delta^{18}\text{O}$ and annual $\delta^{18}\text{O}$ from other Greenland ice cores and from their first principal component (PC1) (Ortega et al., 2014). Initial and end years of individual records are only reported when they deviate from the NEEM ice core time span (1723-2011). The first line is the result for all the available years ; the second line for the same time interval (1767-1966) ; the third line for the same time interval, after detrending. Non significant correlations are displayed in italics. Bold text indicates correlation significant at 95% confidence level or higher.*

Name	Lat.	Lon.	Start Year	End Year	Correlation statistics with NEEM $\delta^{18}\text{O}$
B16	-37.6	73.9		1992	R=0.19 (n=269, p=0.001) R=0.23 (n=206, p=0.000) R=0.23 (n=206, p=0.001)
B18	-36.4	76.6		1992	R=0.20 (n=269, p=0.000) R=0.24 (n=206, p=0.000) R=0.22 (n=206, p=0.001)
B21	-41.1	80		1993	R=0.21 (n=270, p=0.000)

					R=0.16 (n=206, p=0.010) R=0.15 (n=206, p=0.014)
B26	-49.2	77.3		1994	R=0.24 (n=271, p=0.000) R=0.26 (n=206, p=0.000) R=0.25 (n=206, p=0.000)
<u>B29</u>	-43.5	76		1994	R=0.44 (n=271, p=0.000) R=0.47 (n=206, p=0.000) R=0.46 (n=206, p=0.000)
Camp Century	-66.1	77.2		1967	R=0.23 (n=244, p=0.000) R=0.24 (n=206, p=0.000) R=0.23 (n=206, p=0.001)
Crete	-37.3	71.1		1973	R=0.18 (n=250, p=0.002) R=0.19 (n=206, p=0.003) R=0.18 (n=206, p=0.004)
Dye2	-46.2	66.4	1742	1974	R=0.16 (n=233, p=0.008) R=0.17 (n=206, p=0.007) R=0.15 (n=206, p=0.017)
Dye3-3	-43.8	65.2		1978	R=0.25 (n=269, p=0.001) R=0.26 (n=206, p=0.000) R=0.23 (n=206, p=0.001)
Dye 3- 20D	-44.9	65	1767	1984	R=0.24 (n=218, p=0.000) R=0.24 (n=206, p=0.000) R=0.23 (n=206, p=0.001)
<u>GISP2</u>	-38.5	72.6		1987	R=0.30 (n=264, p=0.000) R=0.33 (n=206, p=0.000) R=0.33 (n=206, p=0.001)
GRIP	-37.6	72.6		1979	R=0.16 (n=256, p=0.005) R=0.18 (n=206, p=0.005) R=0.19 (n=206, p=0.003)
MILCENT	-44.6	70.3		1967	R=0.22 (n=244, p=0.000) R=0.26 (n=206, p=0.000) R=0.25 (n=206, p=0.001)

<u>NGRIP</u>	-42.3	75.1		1995	R=0.40 (n=272, p=0.000) R=0.49 (n=206, p=0.000) R=0.48 (n=206, p=0.000)
RENLAN D	-26.7	71.3		1986	R=0.29 (n=263, p=0.001) R=0.18 (n=206, p=0.004) R=0.17 (n=206, p=0.007)
SITE A	-35.8	70.6		1986	R=0.10 (n=261, p=0.053) <i>R=0.09 (n=206, p=0.111)</i> <i>R=0.08 (n=206, p=0.141)</i>
<u>PC1</u>			1761	1966	R=0.48 (n=206, p=0.000) R=0.48 (n=206, p=0.000) R=0.47 (n=206, p=0.000)

Table S2. Correlation statistics between NEEM annual accumulation and annual accumulation records from other Greenland ice cores and from their first principal component (PC1), calculated using the same method as implemented for $\delta^{18}\text{O}$ (Ortega et al., in press). Initial and end years of individual records are only reported when they deviate from the NEEM ice core time span (1723-2011). The first line is the result for all the available years ; the second line for the same time interval (1767-1966) ; the third line for the same time interval, after detrending. Non significant correlations are displayed in italics. Bold text indicates correlation significant at 95% confidence level or higher.

Name	Lat.	Lon.	Start Year	End Year	Correlation statistics with NEEM accumulation
B16	-37.6	73.9		1992	<i>R=0.09 (n=268, p=0.079)</i> <i>R=0.07 (n=206, p=0.141)</i> <i>R=0.07 (n=206, p=0.142)</i>
B18	-36.4	76.6		1992	<i>R=-0.03 (n=268, p=0.286)</i> <i>R=-0.04 (n=206, p=0.283)</i> <i>R=-0.04 (n=206, p=0.277)</i>
B21	-41.1	80		1993	<i>R=0.05 (n=269, p=0.194)</i> <i>R=0.08 (n=206, p=0.137)</i> <i>R=0.07 (n=206, p=0.148)</i>
B26	-49.2	77.3		1994	<i>R=0.10 (n=269, p=0.194)</i> <i>R= 0.07 (n=206, p=0.151)</i> <i>R=0.07 (n=206, p=0.151)</i>
<u>B29</u>	-43.5	76		1994	R=0.35 (n=270, p=0.000) R=0.38 (n=206, p=0.000) R=0.38 (n=206, p=0.000)
<u>Camp Century</u>	-66.1	77.2		1967	R=0.32 (n=217, p=0.000) R=0.38 (n=206, p=0.000) R=0.44 (n=206, p=0.000)
Crete	-37.3	71.1		1973	<i>R=0.02 (n=251, p=0.367)</i> <i>R=0.06 (n=206, p=0.214)</i>

					$R=0.06$ ($n=206$, $p=0.199$)
Dye2	-46.2	66.4	1742	1974	R=0.11 (n=233, p=0.047) R=0.11 ($n=206$, $p=0.054$) R=0.14 (n=206, p=0.024)
Dye3-3	-43.8	65.2		1978	$R=0.03$ ($n=254$, $p=0.335$) $R=0.10$ ($n=206$, $p=0.076$) $R=0.11$ ($n=206$, $p=0.064$)
GISP2	-38.5	72.6		1987	R=0.13 (n=255, p=0.019) R=0.17 (n=206, p=0.009) R=0.17 (n=206, p=0.009)
GRIP	-37.6	72.6		1979	R=0.16 (n=255, p=0.006) R=0.15 (n=206, p=0.014) R=0.15 (n=206, p=0.014)
MILCENT	-44.6	70.3		1967	R=0.18 (n=244, p=0.002) R=0.20 (n=206, p=0.002) R=0.20 (n=206, p=0.002)
<u>NGRIP</u>	-42.3	75.1		1996	R=0.34 (n=271, p=0.000) R=0.38 (n=206, p=0.000) R=0.38 (n=206, p=0.000)
<u>PC1</u>			1761	1966	R=0.39 (n=206, p=0.000) R=0.39 (n=206, p=0.000) R=0.40 (n=206, p=0.000)

Table S3. Statistics of linear correlation between NEEM records, coastal SW Greenland temperature (Vinther et al., 2006), NAO instrumental index (Vinther et al., 2003), AMO records (based on instrumental datasets, AMO1 : (Trenberth and Shea, 2006), AMO2 : (Enfield et al., 2001) ; and based on reconstructions, AMO3 : (Svendsen et al., 2014)). Italics indicate non significant correlation, while bold text indicates correlation significant at 95% confidence level or higher. The time span of each meteorological record is indicated in the left column. The number of years used for correlation analysis depends on the NEEM series (as the accumulation record ends in 2007 and the isotope record ends in 2011). In each cell, the upper statistics are for the raw records, and the lower statistics for detrended records.

	NEEM $\delta^{18}\text{O}$	NEEM accumulation	NEEM deuterium excess
NAO DJFM 1823-2011	R=-0.11, n=189, p=0.061 <i>R=-0.05, n=189, p=0.232</i>	R=-0.14, n=185, p=0.025 R=-0.20, n=185, p=0.003	R=0.21, n=189, p=0.001 R=0.19, n=189, p=0.004
NAO JJAS 1822-2011	R=-0.13, n=189, p=0.034 R=-0.20, n=189, p=0.003	<i>R=-0.06, n=186, p=0.210</i> R=-0.17, n=186, p=0.009	<i>R=0.07, n=190, p=0.176</i> <i>R=0.04, n=190, p=0.272</i>
SW Greenland temperature DJFM 1784-2011	R=0.32, n=199, p=0.000 R=0.22, n=157, p=0.000	R=0.25, n=195, p=0.000 R=0.17, n=153, p=0.000	<i>R=-0.04, n=199, p=0.300</i> <i>R=-0.06, n=157, p=0.217</i>
SW Greenland temperature JJAS 1807-2011	R=0.49, n=182, p=0.000 R=0.44, n=157, p=0.000	R=0.24, n=178, p=0.001 R=0.20, n=153, p=0.006	<i>R=0.13, n=182, p=0.045</i> <i>R=0.06, n=157, p=0.231</i>
AMO1	R=0.17,	R=0.21,	<i>R=-0.11,</i>

1870-2011	n=141, p=0.020 R=0.14, n=141, p=0.045	n=138, p=0.008 R=0.20, n=138, p=0.009	<i>n=141, p=0.098</i> <i>R=-0.10,</i> <i>n=141, p=0.111</i>
AM02 1856-2011	R=0.18, n=156, p=0.013 R=0.20, n=156, p=0.005	R=0.22, n=156, p=0.001 R=0.20, n=152, p=0.006	R=-0.25, n=156, p=0.001 R=-0.24, n=156, p=0.001
AM03 1781-1807	<i>R=0.09,</i> <i>n=206, p=0.092</i> <i>R=0.03,</i> <i>n=206 p=0.424</i>	<i>R=0.03,</i> <i>n=206, p=0.329</i> <i>R=0.01,</i> <i>n=206, p=0.424</i>	R=-0.22, n=206, p=0.001 R=-0.28, n=206, p=0.000

Table S4. Analysis of linear correlation between the first and second principal component of sea level pressure north of 70°N and NEEM records, for two intervals (1870-2010 and 1930-2010), for data at annual resolution (1 year) and smoothed over 3 and 5 years. One asterisk (*) indicates correlation coefficients significant at 95% confidence level. Two asterisks (**) indicate correlation coefficients significant at 99% confidence level.

Sea level pressure north of 70°N	NEEM $\delta^{18}\text{O}$	NEEM deuterium excess	NEEM accumulation
PC1 (Arctic Oscillation) 1870-2010	1 yr: -0.04 3 yr: 0.00 5 yr: 0.07	1 yr: 0.11 3 yr: 0.27** 5 yr: 0.37**	1 yr: -0.15 3 yr: -0.19* 5 yr: -0.15
PC1 (Arctic Oscillation) 1930-2010	1 yr: 0.09 3 yr: 0.29** 5 yr: 0.48**	1 yr: 0.01 3 yr: 0.14 5 yr: 0.29**	1 yr: 0.03 3 yr: 0.11 5 yr: 0.25*
PC2 (Arctic Dipole) 1870-2010	1 yr: 0.09 3 yr: 0.13 5 yr: 0.15	1 yr: 0.08 3 yr: 0.15 5 yr: 0.19*	1 yr: 0.02 3 yr: 0.07 5 yr: 0.15
PC2 (Arctic Dipole) 1930-2010	1 yr: 0.11 3 yr: 0.28** 5 yr: 0.41**	1 yr: -0.06 3 yr: -0.03 5 yr: -0.08	1 yr: 0.12 3 yr: 0.24* 5 yr: 0.38**

Table S5. Statistics of linear correlation between NEEM records, and the four main North Atlantic weather regimes (Ortega et al., in press) in winter (DJFM) and summer (JJAS), for 1900-2011 (isotopes) and 1900-2007 (accumulation). In each cell, the upper statistics are for the raw records, and the lower statistics for detrended records. Asterisks (*) denote correlations which are still significant when considering the period 1960-2011.

Weather regimes 1900-2011	NEEM annual $\delta^{18}\text{O}$	NEEM annual accumulation	NEEM annual deuterium excess
Summer (JJAS)			
NAO+	R=-0.21* , n=112, p=0.015 R=-0.21* , n=112 p=0.013	R=-0.14* , n=108, p=0.013 R=-0.14*, n=108, p=0.073	R=0.11, n=112, p=0.131 R=0.11, n=112 p=0.120
NAO-	R=0.27* , n=112, p=0.002 R=0.29* , n=112 p=0.001	R=0.07, n=108, p=0.235 R=0.08, n=108, p=0.203	R=0.09, n=112, p=0.176 R=0.07, n=112, p=0.231
Atlantic Ridge	R=0.03, n=112, p=0.384 R=0.02, n=112, p=0.407	R=0.12, n=108, p=0.100 R=0.12, n=108, p=0.106	R=0.01, n=112, p=0.441 R=0.02, n=112, p=0.417
Scandinavian Blocking	R=-0.10, n=112, p=0.158 R=-0.10, n=112, p=0.135	R=-0.04, n=108, p=0.347 R=-0.04, n=108, p=0.328	R=-0.20, n=112, p=0.016 R=-0.19, n=112, p=0.020
Winter (DJFM)			
NAO+	R=0.00, n=112, p=0.495 R=-0.01, n=111, p=0.455	R=-0.07 n=108, p=0.245 R=-0.07, n=108, p=0.228	R=0.10, n=111, p=0.153 R=0.10, n=111, p=0.158
NAO-	R=0.03,	R=0.10,	R=-0.08, n=112,

	<i>n=112, p=0.365</i> <i>R=0.04,</i> <i>n=112, p=0.331</i>	<i>n=108, p=0.142</i> <i>R=11,</i> <i>n=108, p=0.133</i>	<i>p=0.221</i> <i>R=-0.03,</i> <i>n=112,</i> <i>p=0.373</i>
Atlantic Ridge	R=-0.19, n=112, p=0.024 R=-0.18 n=112, p=0.027	<i>R=-0.09,</i> <i>n=108, p=0.191</i> <i>R=-0.09,</i> <i>n=108, p=0.188</i>	<i>R=0.03,</i> <i>n=112, p=0.364</i> <i>R=0.06</i> <i>n=112, p=0.268</i>
Scandinavian Blocking	<i>R=0.155</i> <i>n=112, p=0.052</i> <i>R=0.156</i> <i>n=112, p=0.051</i>	<i>R=0.03</i> <i>n=108, p=0.360</i> <i>R=0.04</i> <i>n=108, p=0.352</i>	<i>R=-0.05</i> <i>n=112, p=0.298</i> <i>R=0.00</i> <i>n=112, p=0.479</i>

Figure S1 : 1st Principal Component (PC1, left) and 1st Empirical Orthogonal Function (EOF, right) of annually resolved snow accumulation records from Greenland ice-cores. All time-series are standardised with respect to their common period (1761-1966) before performing the Principal Component Analysis. The position of NEEM is marked by a purple star. The same methodology was initially applied to $\delta^{18}\text{O}$ records, we refer the reader to (Ortega et al., 2014). The leading mode of snow accumulation across Greenland depicts a monopole-like pattern, with maximum values at Summit (GRIP-GISP2), and particularly low values in the vicinity of NEEM (e.g. B26).

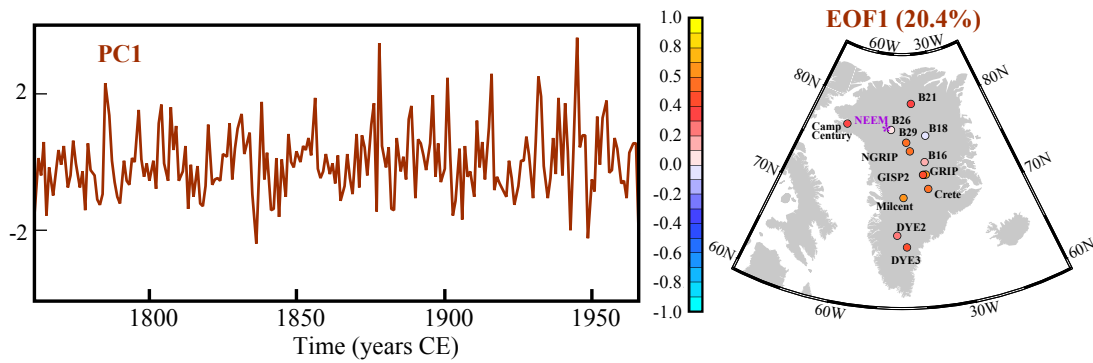
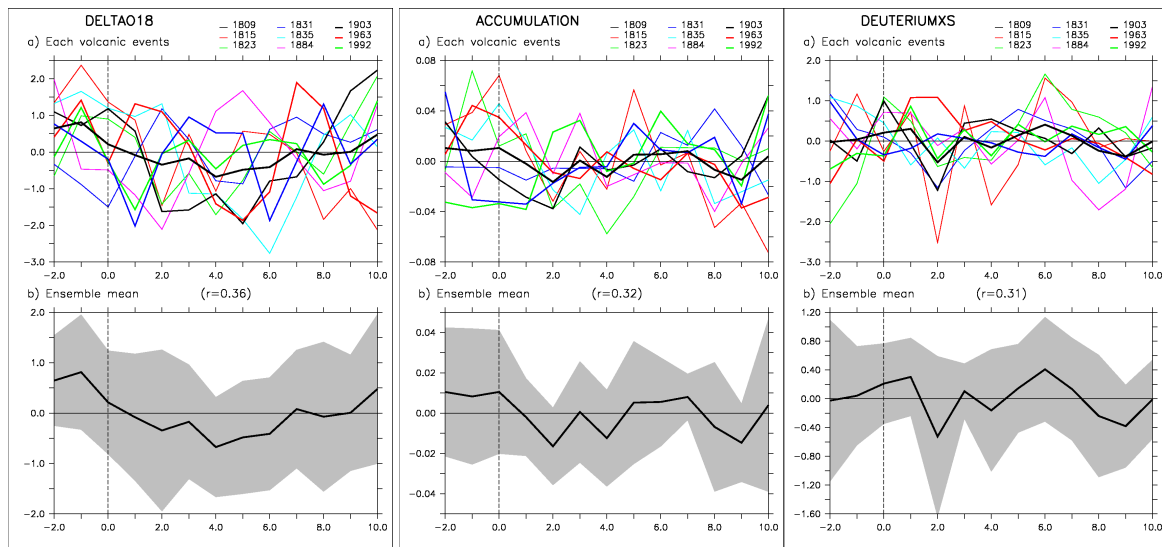


Figure S2 : Individual (upper panels) and composite (lower panel) response of NEEM $\delta^{18}O$ (left), accumulation (middle) and deuterium excess (right panels) following major volcanic eruptions of the 19th and 20th centuries. The correlation coefficient reported on each lower panel is the average correlation coefficient between the ensemble mean and the response following each volcanic event.



References

Enfield, D. B., Mestas-Nuñez, A. M., and Trimble, P. J.: The atlantic multidecadal oscillation and its relation to rainfall and river flows in the continental u.S, *Geophys Res Lett*, 28, 2077-2080, 10.1029/2000gl012745, 2001.

Ortega, P., Swingedouw, D., Masson-Delmotte, V., Risi, C., Vinther, B., Yiou, P., Vautard, R., and Yoshimura, K.: Characterizing atmospheric circulation signals in greenland ice cores: Insights from a weather regime approach, *Clim Dynam*, 1-21, 10.1007/s00382-014-2074-z, 2014.

Ortega, P., Swingedouw, D., Masson-Delmotte, V., Risi, C., Vinther, B., Yiou, P., Vautard, R., and Yoshimura, K.: Characterizing the atmospheric signals in greenland ice cores: Insights from the weather regime approach, *Clim. Dyn.*, in press.

Svendsen, L., Hetzinger, S., Keenlyside, N., and Gao, Y.: Marine-based multiproxy reconstruction of atlantic multidecadal variability, *Geophys Res Lett*, 41, 2013GL059076, 10.1002/2013gl059076, 2014.

Trenberth, K. E., and Shea, D. J.: Atlantic hurricanes and natural variability in 2005, *Geophys Res Lett*, 33, L12704, 10.1029/2006gl026894, 2006.

Vinther, B. M., Andersen, K. K., Hansen, A. W., Schmith, T., and Jones, P. D.: Improving the gibraltar/reykjavik nao index, *Geophys Res Lett*, 30, 2222, 10.1029/2003gl018220, 2003.

Vinther, B. M., Andersen, K. K., Jones, P. D., Briffa, K. R., and Cappelen, J.: Extending greenland temperature records into the late eighteenth century, *Journal of Geophysical Research: Atmospheres*, 111, D11105, 10.1029/2005jd006810, 2006.